ARTICLE NO. 78-1138

Supercritical Airfoil Technology in Compressor Cascades: Comparison of Theoretical and Experimental Results

H. E. Stephens*
Pratt & Whitney Aircraft Group, East Hartford, Conn.

A shockless supercritical compressor blade designed with an inverse hodograph procedure has been tested in cascade. Comparisons of the measured performance results with those of a conventional cascade tested at the same design conditions are presented. The supercritical design is superior for this advanced application in terms of both reduced losses and increased incidence range. Results of the numerical simulation of the supercritical cascade test conditions using a transonic potential flow solution show good agreement between measured and computed velocity distributions. The ability to design, test, and analyze supercritical cascades is demonstrated through comparisons with detailed experimental results.

Nomenclature

a = sound speed
AVDR = axial velocity density ratio = streamtube inlet area/exit area
b_x = airfoil axial chord = $C\cos\alpha_s$
C = airfoil chord
D_F = diffusion factor = $(1 - W_2/W_1) + \tau/C[(W_1\cos\beta_1 - W_2\cos\beta_2)/2W_1]$
M = Mach number
P = static pressure
P_t = total pressure
q = velocity
s = arc length
U, V = velocity components along x,y
W = velocity
x,y = rectangular coordinate directions
Z = loss coefficient = $(P_{t2} - P_{t1})/(P_{t1} - P_1)$
α_s = surface chord angle
β = air angle measured from tangential
θ = boundary layer momentum thickness
τ = cascade gap

Subscripts

1 = cascade inlet plane
2 = cascade exit plane
x,y = $\partial/\partial x$, $\partial/\partial y$

Introduction

THE ultimate goal of advanced compressor designs is to obtain highly loaded, low loss blading capable of achieving high stage efficiency over a wide range of operating conditions. Potential improvements in compressor aerodynamics have become especially important as a result of an increasing interest in fuel conservation and other economic considerations of airline operations. The development of efficient, highly loaded compressor stages can lead to reduced thrust specific fuel consumption and perhaps a reduction in overall engine size and weight.

One area of particular interest at the present time is the aerodynamic performance improvement of compressor blades operating with high subsonic inlet velocities. Conventional airfoils operating in the transonic regime are usually characterized by locally supersonic velocities extending over a portion of the suction surface and terminating in strong shocks. The resulting high losses are combinations of shock loss and increased viscous loss induced by the shock/boundary-layer interaction. A realization of the potential gain that would result from shock-free transonic designs has led to much work on the development of supercritical airfoils capable of sustaining large regions of controlled supersonic flow with essentially shock-free recompression.

The value of supercritical airfoils has been recognized in isolated airfoil applications since the early 1960's. A substantial amount of information has been compiled describing the development of supercritical airfoils for high lift wing sections. Wu and Moulden[1] presented a survey of transonic aerodynamics including both a synopsis of the historical development of the subject and a review of the current status of research, both analytical and experimental, in transonic flows.

Much of the early work in this field was primarily empirical in approach. Both Pearcey and Whitcomb developed pressure distributions that included regions of controlled supersonic flow. Lock and Fulker[2] describe the experimental modification of a National Physics Laboratory (NPL) airfoil in an attempt to extend low loss performance into regions of transonic inlet velocities. These empirical developments established the groundwork for supercritical airfoil technology.

In recent years advancements in computational solutions to the transonic flow equations have provided a basis for analytical techniques to improve the design of transonic airfoils. These analytical methods include procedures for both the direct or analysis problem and the inverse or design problem. In the analysis method, the airfoil geometry and a sufficient set of boundary conditions are specified and the resulting flowfield is computed. The inverse procedure starts with a specified pressure distribution and generates an airfoil geometry which will produce the intended lift distribution. One such inverse procedure is the complex hodograph solution developed by Garabedian et al.[3,4] This procedure obtains an airfoil shape from a given pressure distribution by solving the compressible, two-dimensional potential flow equations by use of complex characteristics after mapping the flowfield into the complex hodograph plane. Corrections for viscous boundary-layer effects are incorporated by including an iteration between the boundary-layer and inviscid potential flow calculations. The validity of this design procedure has been demonstrated in tests of isolated airfoils designed by Korn and Garabedian and tested by the National Research Council of Canada.[5]

Presented as Paper 78-1138 at the AIAA 11th Fluid and Plasma Dynamics Conference, Seattle, Wash., July 10-12, 1978; submitted July 31, 1978; revision received Jan. 17, 1979.

Index categories: Transonic Flow; Aerodynamics; Airbreathing Propulsion.

*Senior Analytical Engineer. Member AIAA.

The documented success of these supercritical wing sections appeared to offer a potential for improving compressor efficiency, since many blade sections in axial flow compressors operate with high subsonic inlet relative Mach numbers. An optimization of these blade sections could lead to substantial improvements in stage loading capability, reductions in stage loss, and perhaps even a reduction in engine weight. This latter effect could result from a reduction in the total number of blades requird to provide a specified pressure rise due to the inherent high loading capabilities of supercritical airfoils.

In order to investigate the extent to which supercritical advantages may be used in compressor applications, Bauer, Garabedian, and Korn (BGK) extended their design procedure to facilitate the design of supercritical compressor cascades. Under contract to Pratt & Whitney Aircraft (P&WA), Korn designed a highly loaded supercritical cascade that was intended to operate with low loss at the transonic design point.

A comprehensive test of this airfoil was conducted in the Transonic Cascade Facility at the DFVLR Institut fur Luftstrahlantriebe located in Porz-Wahn, West Germany. The objectives of this test were twofold: first, demonstrate the accuracy of the inviscid transonic design system through a comparison with experimental data; and second, investigate the performance of an analytically designed airfoil over a wide range of operating conditions. A test of a double circular arc (DCA) profile was also performed at the DFVLR in order to provide a performance comparison with a more conventional airfoil. Use of the same facility for both tests provided a consistent set of comparison data independent of tunnel effects.

The experimental results for the supercritical and DCA cascades at the design conditions are reported in this paper. Comparisons between calculated and experimental velocity distributions for the supercritical cascade at the design point are also presented. The accuracy of the numerical methods and the successful attainment of essentially shock-free supersonic diffusion in compressor cascades are substantiated with detailed experimental data.

General Considerations of Turbomachinery Applications

In discussing the use of supercritical airfoils in compressors it is important to emphasize that compressor geometries present additional flow complexities not encountered in isolated airfoil operation. Hence, supercritical airfoil technology developed in the aircraft industry may not be directly translated to turbomachinery applications. For example, compressor blade rows are subject to boundary conditions that are more similar to those of diffusers than of isolated airfoils. Adjacent blade surfaces may restrict the full exploitation of the supercritical concept, since transonic flow disturbances are propagated in a direction normal to the mean flow. This effect requires special consideration because compressors are prone to channel choking, which may be greatly aggravated by improper design of the supersonic region. It should be noted that there are additional complexities in compressor flows that are more severe than in isolated airfoil applications. These include three-dimensional, viscous, and unsteady aerodynamic effects.

The development of improved airfoil aerodynamics for gas turbines is often accomplished by first testing a new airfoil design in a stationary, linear cascade arrangement. This is done because two-dimensional or quasi-three-dimensional flowfield calculations are usually employed in the design system. The incorporation of fully three-dimensional calculations has not yet been realized. In addition, the cost of operating linear cascades is only a fraction of that required to obtain rotating compressor data. The ease of instrumentation and the acquisition of detailed performance information also recommend this method for specialized aerodynamic investigations.

While the linear cascade arrangement does not provide information about the three-dimensional or rotational effects on the performance of an airfoil design, it is essential for verification of the accuracy of the design calculations, both inviscid and viscous. Once confidence in these elements of the design system has been established, the study of the effects of other flowfield complexities on the designed airfoil can be addressed.

BGK Design System

The particular design method to be outlined here is the inverse calculation for shock-free supercritical cascades developed by Bauer, Garabedian, and Korn. Because detailed descriptions of this method have been presented elsewhere,[6] no attempt will be made to outline the specific formulation of the governing eqution, or the differencing techniques used in their solution. However, a few of the pertinent details of the design system will be presented.

For the steady flow of an isentropic gas in two dimensions, the continuity, momentum, and energy equation may be combined with the aid of the equation of state to arrive at a single expression describing the flow:

$$(a^2 - U^2)\,U_x - UV(U_y + V_x) + (a^2 - V^2)\,V_y = 0$$

The solution of this equation is complicated by the fact that it is not only nonlinear, but also of mixed type for transonic flows, i.e., hyperbolic over some portion of the flowfield and elliptic over the rest. In order to overcome the first difficulty, the equation is linearized by the introduction of the hodograph transformation, which interchanges the roles of the independent (x,y) and dependent (U,V) variables. This succeeds in reducing the equation to a set of linear, first-order partial differential equations.

Use of the method of characteristics is well established for supersonic flow. The present method uses analytical continuation into the four-dimensional domain of two independent complex variables to permit the definition of complex characteristic coordinates for the case of subsonic flow as well. The domain of integration is mapped conformally into the unit circle in the hodograph plane of one of these coordinates. It is possible to formulate a boundary-value problem on the unit circle which is well posed even in the case of transonic flow.

The general solution is obtained by solving the complex initial-value problem numerically by constructing paths of integration in the complex characteristic planes and using parameters along these paths as real independent variables. The most important restriction on the integration paths is that the two-dimensional surface they define circumvent the two-dimensional sonic surface where the canonical equations become singular. Special care is taken in defining the integration paths in order to avoid this and other numerical difficulties. This solution provides a procedure to arrive at an airfoil on which the speed is prescribed as a function of arc-length.

Viscous effects are incorporated into the design procedure by including an iteration with a turbulent boundary-layer calculation based upon the von Kármán integral equation formulation. The output speed distribution is used to compute the displacement thickness, loss, and the value of the skin friction along the airfoil. The displacement thickness is subtracted from the inviscid profile coordinates to insure that a sufficiently thick blade has been designed, particularly in the vicinity of the trailing edge. If not, the closure conditions for the design procedure are altered and the case is rerun. The recompression rate specified for the suction side speed distribution is maximized by following the notion of the Stratford criterion,[7] which estimates the maximum diffusion rate that a turbulent boundary layer can withstand without separating. In the BGK method, the value of a separation

parameter:

$$\text{SEP} = -\frac{\theta}{q}\frac{dq}{ds}$$

is maintained at a constant value, typically 0.002, along the blade surface by adjusting the input speed distribution. Separation of the boundary layer is signaled by a value of SEP > 0.004. A completely turbulent boundary layer is calculated by selecting the transition point based on experience and then beginning the turbulent boundary layer at that point without regard to history effects. A laminar/transition/turbulent boundary-layer technique[8] has been used at P&WA to perform the final adjustment of the computed airfoil to obtain metal coordinates for manufacture.

Description of the Cascades

The unique feature of supercritical airfoils is a region of controlled supersonic velocity on the airfoil surface followed by an essentially isentropic compression to the trailing edge velocity. These airfoils not only eliminate shock losses at the design condition, but also avoid the penalty of increased viscous losses caused by shock/boundary layer interactions. The ability to control the supersonic region permits an increase in the induced circulation which can, in turn, lead to a reduction in the number of compressor blades required to achieve a specified pressure rise. Fewer blades imply lighter stages and lower fabrication and maintenance costs. The potential benefits that supercritical airfoils offer warrant the careful investigation of the concept.

Under contract to P&WA, Korn designed a highly loaded supercritical cascade intended to operate with low loss at the transonic design point. The design conditions included an inlet Mach number of 0.78, flow turning of 25 deg, and a diffusion factor (D_F) of 0.66. The design Mach number distribution and the displacement surface airfoil geometry are shown in Fig. 1. The suction side velocity was designed with supersonic flow over 36% axial chord, a peak Mach number of 1.22, and an isentropic compression to the exit Mach number. The high blade loading was primarily a consequence of the large gap/chord ratio (1.2) which resulted from a limitation implicit in the particular coordinate mapping scheme used in the BGK computational procedure. The suction surface is contoured to permit shock-free diffusion at a maximum rate without causing separation of the boundary layer. The pressure side was designed to provide a substantial amount of rear loading by keeping higher pressure on the lower surface while avoiding any additional disturbance of the more sensitive suction side boundary layer. This additional aft loading resulted in an airfoil thickness distribution that reached a minimum at 80% axial chord and then flared out again as the trailing edge was approached. Since this was to be a test of an analytical procedure, the practical arguments against producing and maintaining such a blade were postponed for future consideration and the airfoil was tested as designed.

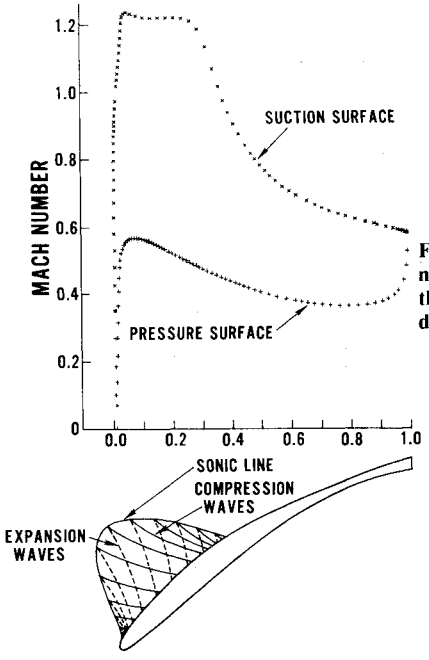

Fig. 1 Design Mach number distribution for the supercritical cascade designed by Korn.

In spite of the large amount of cascade data compiled by NACA and by P&WA, performance data for conventional airfoils tested under the particular design conditions characteristic of this supercritical cascade were not available to the author. To fill this void a 48-deg camber double circular arc (DCA) airfoil intended to produce the same inlet and exit conditions as the supercritical cascade was designed. The gap/chord ratio for the DCA was selected to be the same as that for the supercritical, in spite of the fact that the resulting blade loading was much higher than would normally be employed for this type of airfoil. This cascade was also tested at the DFVLR in order to provide a consistent set of comparison data. The two cascade geometries are shown in Fig. 2.

Description of the Test Facility

The facility used in this investigation was built by NACA in the early 1950's and transferred to the DFVLR in 1963.[9] The transonic cascade tunnel is a closed loop, continuously running facility with variable nozzle and variable test section height. This tunnel is unique in its extensive endwall boundary-layer control system and its substantial vacuum capacity, which can remove as much as 50% of the total tunnel flow through various bleed schemes. These provisions were essential for controlling the secondary flows induced by the strong gapwise pressure gradients of the supercritical cascade. The dry air is delivered by a set of compressors with a total installed power of 5000 KW (3728 hp) and a mass flow of up to 20 kg/s (44 lbm/s). The tunnel test section height is variable between 150 and 450 mm (5.9 and 17.7 in.), and the span is 167 mm (6.6 in.). This gives an aspect ratio of 2.36 for a blade chord of 71 mm (2.8 in.). The tunnel Reynolds number can be varied from 4×10^5 to 4×10^6 by changing the settling chamber pressure. The nozzle is half-symmetrical, with a variable shape for the upper half and a variable height adjustment for the flat lower half. This arrangement provides a Mach number range from 0 to 1.4. The Mach number is uniform over the test section height within ±1.5% of the maximum, and the turbulence level in the inlet is 0.5% ±0.2% for an inlet Mach number of 0.3 to 0.7.

A schematic representation of the cascade tunnel and boundary-layer control system is shown in Fig. 3.

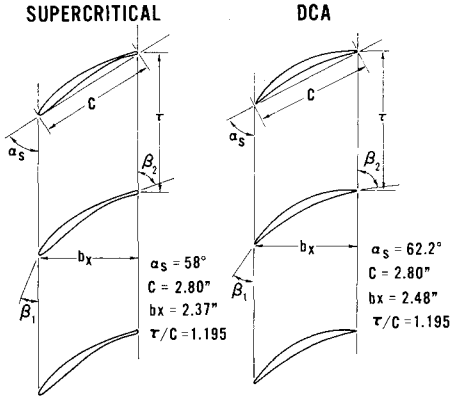

Fig. 2 Comparison of the supercritical and DCA cascade geometries.

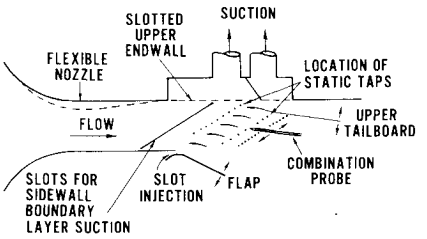

Fig. 3 Schematic diagram of the DFVLR transonic cascade facility.

The upper wall of the test section is slotted and equipped with suction to improve the inlet flow conditions. Additional suction capability is available for boundary-layer removal ahead of the test section (slots in the sidewalls reaching from nozzle top to bottom wall) and through chordwise-slotted cascade endwalls within the blade pack. The tunnel top endwall flow is separated from the cascade core flow by a tailboard system that is hinged at the trailing edge of the outermost cascade blade.

The inlet air angle is measured at the same gapwise locations for three consecutive blade channels. The downstream traverse probe measures a combination of pressures to give both total and static pressure as well as flow angle for the complete wake traverse information.

Data Acquisition/Reduction System

A demonstration of the accuracy of the inviscid transonic design system through comparisons with measured cascade data required precise control of the experimental setup to insure that the design conditions were matched as closely as possible. In order to insure that the measured performance was obtained under periodic flow conditions, several procedures were observed. Tunnel periodicity was checked by comparing the inlet flow angle as measured at three adjacent gap positions and by observing the inlet and exit static pressure distributions displayed on manometer boards located in the test cell control room. The exit traversing probe was operated in a continuously running mode, enabling three adjacent blades to be traversed in a reasonable length of time. The resulting wake profiles were displayed on an $X-Y$ plotter to check blade wake consistency. In addition, wake traverses at various spanwise locations were made to guarantee that an acceptable portion of the blade was operating under two-dimensional conditions. Adjustments were made to the movable bottom endwall, tailboard settings, and extensive boundary-layer control vacuum system to obtain periodic flow conditions.

Complete information for each test point was recorded by an automatic data acquisition system and stored on magnetic tape by a digital computer system used to control the data sequencing. This information included plenum conditions, inlet static pressure and flow angle information, blade surface pressure distributions, and downstream traverse data. The wake traverse system employed a combination probe that provided flow angle and both total and static pressure information. The traverse system was operated in a stepping mode when making loss measurements in order to insure that the probe had sufficient time to accurately resolve total pressure measurement in portions of the wake where strong flow gradients exist.

An on-line data reduction system provided a summary of computed performance information that was displayed real-time on a remote computer terminal equipped with a scope display. In addition, the design blade pressure distribution was displayed on the scope along with the measured pressures so that an immediate evaluation could be made of the test point results. A complete off-line data reduction system provided detailed test information, including corrections for probe calibrations and stream-thrust averaging of the loss information.

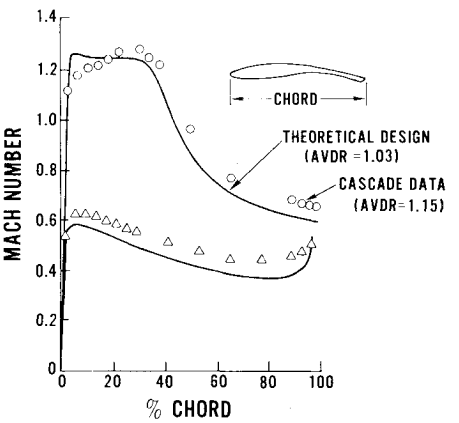

Fig. 4 Comparison of theoretical and measured Mach number distributions for the near-design test condition of the supercritical cascade.

Test Results

To check the design method accurately, the supercritical cascade blades were heavily instrumented with surface pressure taps. A practical consideration, the blade thickness, dictated that three separate airfoils be instrumented rather than just one. One airfoil was pressure tapped chordwise on the suction surface, a second on the pressure surface, and a third was instrumented spanwise on both surfaces at only a few chordwise locations. The pressure and suction instrumented blades were arranged in cascade so that they recorded the flow within a common blade passage. When attempting to match the design point a plot of the theoretical pressure distribution was displayed on a scope along with the measurements. The tunnel conditions were optimized to obtain the best possible match to the design surface velocities. It was felt that the blade loading distribution rather than specified inlet and exit conditions should be the criterion for comparison purposes since tunnel effects, both viscous and three-dimensional, might alter the blade loading. A parametric variation of inlet conditions demonstrated that the best match to the design pressure distribution was obtained by operating the cascade at 2 deg positive incidence and with approximately 15% streamtube contraction between the upstream and downstream measurement planes. The resulting Mach number distribution for this near design condition is shown in Fig. 4, along with the theoretical values. The measurements in the leading edge region of the suction surface do not exhibit the sharpness of the theoretical design. This has been shown to be the result of variations in blade geometry as manufactured. The velocities on both surfaces except in the region just mentioned are higher than intended. This is a result of streamtube height variation and will be discussed in detail in a following section. It should be noted that the BGK inverse procedure is purely two-dimensional and includes no effect of streamtube height variation in the analysis. It is interesting to note that the theoretical compression rate specified for the suction surface based on the Stratford criterion has been attained in the test, and as a result the blade viscous losses are very low.

The question of whether or not shock-free supercritical flow was actually achieved in the cascade test cannot be answered conclusively based upon the data available. However, all indications are that isentropic, or nearly shock-free diffusion was attained. In particular, the intended recompression rate was matched at the near-design test condition and the boundary layer did remain attached throughout its diffusion. It is difficult to imagine that the agreement would be so good if some significant disturbance of the shock-free flow had occurred.

A comparison of the DCA and supercritical cascade performance results are shown in Figs. 5 and 6. Figure 5 shows a

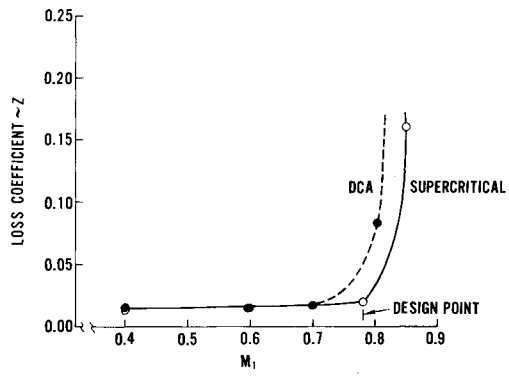

Fig. 5 Comparison of minimum loss performance for the supercritical and DCA cascades.

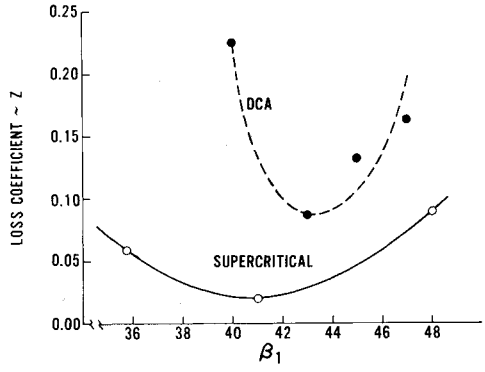

Fig. 6 Comparison of supercritical and DCA loss variations with inlet flow angle at design inlet Mach number.

comparison of the drag rise characteristics for both cascades. The losses shown are the minimum loss values for each inlet Mach number condition. Up to a Mach number of 0.7 the two cascades have nearly the same minimum loss values; however, at higher speeds the DCA loss increases dramatically. The supercritical blade maintains its low loss up to the design condition of $M_1 = 0.78$, although beyond this point the loss increases abruptly. It should be reiterated here that the supercritical blade was optimized at this design condition by specifying a recompression rate which would just barely keep the suction surface boundary layer attached. It should not be concluded that these airfoils do not possess Mach number range. On the contrary, the low measured losses up to the design inlet velocity indicate that range can be insured by selecting the design point above the expected operating condition, or by specifying a less aggressive diffusion rate at the design point in order to provide good off-design performance. Figure 6 demonstrates the incidence range benefit of the supercritical cascade. The measured incidence range of the supercritical airfoil was greater than the DCA over a broad range of inlet Mach numbers.

Description of the Transonic Analysis Program

A computer program to analyze mixed transonic cascade flows has been developed by Ives and Liutermoza[10] of P&WA. Briefly, this calculation procedure uses a series of conformal transformations to map the region exterior to the cascade blades into a rectangular computational domain. This mapping, for a uniform mesh in the computational domain, produces a grid in the physical plane that is automatically dense near the leading and trailing edges of the blades where a fine grid is required to accurately resolve the details of large gradients in flow properties. The grid is relatively uniform across the channel where, except for shock waves, there are only moderate flow gradients. Regions far upstream and far downstream of the cascade map into a point in the computational plane so that a sparse grid is obtained at locations far from the cascade plane where flow gradients are small. The periodicity condition is reduced by the mapping to a single continuity condition. The blade surface boundary condition of zero normal velocity is satisfied to second-order accuracy since the blade becomes a coordinate line in the mapped computational plane. The full transonic potential equation is solved using a fully second-order accurate finite difference procedure in which central differences are used in subsonic regions and a rotated backward difference scheme is used in the supersonic zones. Line relaxation is used to solve the finite differences without the need of explicit numerical damping terms. Streamtube contraction effects are incorporated in the analysis through the specification of streamtube height variation in any desired fashion from the upstream to downstream boundary condition planes.

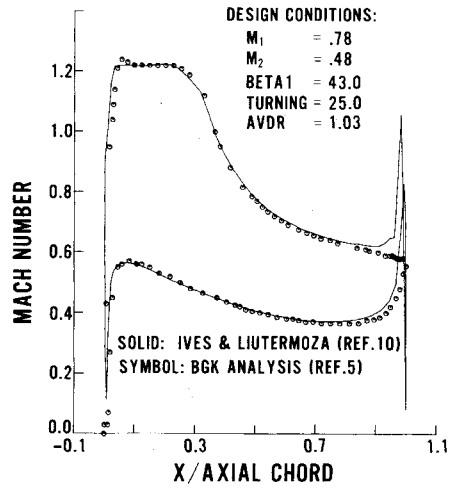

Fig. 7 Comparison of computed Mach number distributions for the supercritical cascade design conditions.

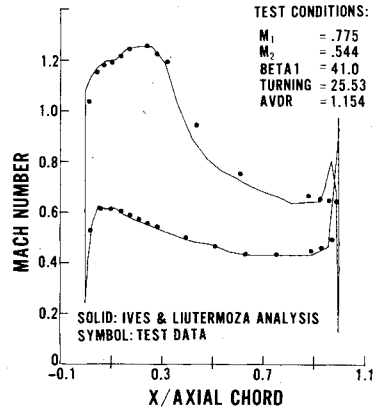

Fig. 8 Comparison of measured and computed Mach number distributions for the near design test condition.

The accuracy of the calculation has been demonstrated[10,11] through comparisons with other numerical methods. As further demonstration of its validity, this program was used to compute the flow about the supercritical cascade designed by Korn. The computed Mach number distributions for the theoretical design conditions are shown in Fig. 7. The agreement between the two inviscid calculations is excellent except in the region very close to the trailing edge. This local discrepancy in the P&WA analysis is a consequence of the inviscid flow accelerating around the blunt trailing edge to reach the rear stagnation point. In the BGK analysis the blade does not close but rather extends at a constant thickness to infinity as a result of the particular form of the boundary conditions applied at the trailing edge. With this minor exception, the two solutions are virtually identical.

Numerical Simulation of the Cascade Results

While comparisons with analytical results are important, the ability to compute flows as they exist in cascades or rotating machinery is the ultimate proof of a calculation's usefulness. Comparisons with experimental results are especially difficult due to uncertainties not only in the numerical results but in the measured test data as well. Several of the supercritical cascade test conditions have been computed to demonstrate the viability of the program as an accurate analysis tool for transonic flows with imbedded regions of supersonic velocities. A simulation procedure developed through a consideration of the physics of the actual flowfield has been established. This procedure includes compensation for blade viscous effects, the wake mixing process, and the distribution of streamtube height in the potential flow solution. Once the simulation procedure was established it was applied uniformly for all of the test conditions considered. A brief description of the details of the simulation procedure is presented in the Appendix.

The minimum loss near design test condition was used for the initial comparison work. This test point, as mentioned previously, differed from the theoretical design conditions in both inlet angle (2-deg positive incidence) and streamtube contraction (approximately 15%). Figure 8 shows a plot of the computed and measured Mach number distributions. The first observation to be made is the improved agreement on the pressure and suction surfaces that resulted from the inclusion of the measured streamtube contraction in the analysis program. The second feature of note is the good match in the leading-edge portion of the suction surface. As shown in Fig. 4, the test data diverged from the design Mach number distribution in this region. The cause of this discrepancy was traced to improper blade geometry in the supercritical region. Shadowgraphs of the instrumented airfoils used in the test were digitized and used as geometry input for the potential flow solution. The combination of proper blade geometry and inclusion of streamtube height provided a good match with the measured data.

Once the simulation procedure has been demonstrated successfully at the design point, it remained to determine the extent of its usefulness for off-design conditions. A representative set of test results, including positive and negative incidence conditions for both subcritical and supercritical flows, was selected for use in these simulations. In all cases the results of the numerical computations agreed with the measured pressure distributions.

Conclusions

The comprehensive tests of the supercritical and DCA cascades succeeded in satisfying the goals of the experiment. The validity of the BGK inverse design program has been demonstrated through comparisons with the measured test results. Although an exact duplication of the theoretical design pressure distribution was not achieved, the differences have been shown to result from improper blade geometry and a failure to include streamtube contraction effects in the inverse design program. The supercritical cascade operated with essentially shock-free recompression at the near-design test condition. The intended recompression rate was achieved and the boundary layer remained attached throughout its diffusion.

A comparison of the supercritical and conventional DCA performance results clearly demonstrates the superiority of the supercritical cascade in terms of both reduced loss and incidence range improvement for this particular application. The implications for designers of advanced turbomachinery are significant. The good aerodynamic performance of this highly loaded cascade offer the possibility of reducing stage weight by decreasing the number of airfoils employed to obtain a specified pressure rise. It should be mentioned that the peculiarities of the particular geometry used in this investigation are not necessary in order to attain supercritical flow. The blunt trailing edge and the very thin blade thickness at 80% axial chord have both been removed in subsequent designs without impairing the overall performance of the designed airfoil.

The good agreement between the measured velocity distribution and the corresponding velocities computed using the transonic cascade analysis program substantiates the accuracy of the potential flow solution for mixed transonic flows. The simulation procedure used to account for viscous effects seems to be adequate for the cases considered. The success of the simulation procedure demonstrates that the method can be employed in the design and analysis of nonstandard airfoil sections. This should permit compressor designers to improve the aerodynamic performance of their machines by employing airfoils that are individually tailored to the design requirements.

The success of this preliminary test has demonstrated an ability to design and analyze mixed transonic flows. The good agreement between analytical and experimental results has justified the further development of supercritical airfoil technology for turbomachinery applications.

Appendix: Details of the Simulation Procedure

Blade Geometry

Theoretical shock-free supercritical flow is achieved through a precise contouring of the blade surface which causes the left running expansion waves to be reflected as right running compression waves from the sonic line, as shown in Fig. 1. If the recompression is to be isentropic the surface must be convex throughout the supersonic region. If any portion of this region is concave or flat the compression waves will coalesce at some point to form a shock. As a result, a shock cannot be explicitly associated with the blade contour in the immediate vicinity of the discontinuity since the coalescence may be a result of nonideal expansion waves generated near the blade leading edge. During the test the suction and pressure surface measurements were made on two separate blades due to the impracticality of instrumenting both sides of the same airfoil. Both of the instrumented blades were shadowgraphed and these tracings were digitized for geometry input for the potential flow solution. As previously mentioned, this difference between the intended profile and that actually manufactured accounted for the leading edge mismatch of Fig. 4. The importance of using an accurate description of the blade profile cannot be overemphasized because of the nature of the shock-free supercritical concept.

Blade Boundary Layer Modeling

Blade viscous effects were included in the inviscid calculation by superimposing the computed boundary layer displacement thickness on the airfoil metal coordinates. This distribution was obtained by using the measured velocity distribution to run a two-dimensional, compressible laminar/turbulent boundary layer calculation.[12] The validity of this calculation has been verified through comparisons with the results of other viscous calculations and measured test data. The practice of using the measured pressure distribution to run the viscous calculation is valid only for low loss, unseparated cases. In a fully separated flow, the measured velocity downstream of the separation point remains constant. This results in a computed boundary layer which would appear well behaved since the input data do not reflect an adverse gradient. The large sustained pressure gradients in the measured data for the cases considered (e.g., Fig. 8) show no evidence of separation. The proper procedure would involve an iteration between the inviscid and viscous calculations rather than simply using the measured velocity distribution to calculate the displacement thickness of the boundary layer. This has, in fact, been done in subsequent work with no

appreciable alteration of the results. Again the low loss associated with this particular airfoil limit the error introduced with the former method.

Laminar Separation Bubble Calculation

A laminar separation bubble calculation/correlation[13] was used to check the length of a laminar separation bubble and the extent to which it might alter the velocity distribution for the near-design case. This correlation is based on low speed data and has not been proven to be valid under these high velocity conditions. Nevertheless, the correlation was checked and the bubble length was estimated to be very short (less than 2% chord) due to the high Reynolds number of the blade (10^6 based on M_1 and chord) and low turbulence level ($\sim 1/2\%$). The correlated increase in momentum thickness across the bubble was used to restart the viscous calculation in a turbulent mode at the point of the predicted laminar bubble. The differences in the computed boundary-layer properties from those calculated with the natural transition option were negligible. Additional support for this idea that a bubble, if present, had very little effect on the blade flow is provided by the fact that the measured velocities do not reflect any plateau of constant velocity near the start of the adverse gradient as is usually characteristic of bubble separations.

Boundary Conditions for the Inviscid Analysis

A compressible unmixing calculation, similar in nature to the analyses of Lieblein[14] and Stewart[15] was used to arrive at equivalent inviscid exit conditions compatible with the potential flow solution. This unmixing process is based upon a simple one-dimensional consideration of the tangential and axial momentum equations, together with the continuity relation. The unmixing calculation removes the wake mixing effects (additional flow deviation and static pressure rise) not modeled in the inviscid calculation and replaces them with new exit conditions and additional streamtube contraction to satisfy continuity. The inlet conditions measured in the cascade tests were used without modification to set the far upstream boundary conditions.

Streamtube Contraction Distribution

The proper scheduling of streamtube contraction in the inviscid analysis is by far the most nebulous consideration since it varies not only chordwise but also gapwise and there are insufficient test data to compute a streamtube height at individual points within the flowfield. A parametric study of distribution schemes was conducted to determine the best match to the measured results. A linear variation of streamtube height applied between the upstream and downstream measurement planes used in the DFVLR cascade tunnel provided a good match to the measured blade velocity distributions. The fact that such a straightforward scheduling gave a good representation of the measured velocity distribution must be attributed at least in part to the excellent endwall boundary layer removal system employed in the DFVLR tunnel. Total pressure loss surveys at various spanwise positions documented uniform loss conditions over the majority of the airfoil. In addition, surface flow visualization confirmed only small amounts of cross-flow on the suction surface. As a result, the linear variation of streamtube height used in the inviscid analysis provided excellent agreement with the measured data.

Acknowledgment

The author wishes to thank Pratt & Whitney Aircraft Group, Division of United Technologies Corporation, for permission to publish this paper. He is indebted to P. Garabedian, D. Korn, and D. Ives for their help with the computational results. H. Starken, P. Schimming, and J. Renken of the DFVLR were essential to the success of the experimental results. Of the many people at P&WA who contributed to this work, special thanks are due J. P. Nikkanen for his many helpful suggestions.

References

[1] Wu, J. M. and Moulden, T. H., "A Survey of Transonic Aerodynamics," AIAA Paper 76-326, San Diego, Calif., July 1976.

[2] Lock, R. G. and Fulker, J. L., "Design of Supercritical Aerofoils," *Aeronautical Quarterly*, Nov. 1974, pp. 245-265.

[3] Bauer, F., Garabedian, P., and Korn, D., "Supercritical Wing Sections," *Lecture Notes in Economics and Mathematical Systems*, Vol. 66, Springer-Verlag, New York, 1972.

[4] Bauer, F., Garabedian, P., Korn, D., and Jameson, A., "Supercritical Wing Sections II," *Lecture Notes in Economics and Mathematical Systems*, Vol. 108, Springer-Verlag, New York, 1975.

[5] Kacprzynski, J. J., Ohman, L. H., Garabedian, P. R., and Korn, D. G., "Analysis of the Flow Past a Shockless Lifting Airfoil in Design and Off-Design Conditions," Aeronautical Report LR-554, National Research Council of Canada, Ottawa, 1971.

[6] Bauer, F., Garabedian, P., and Korn, D., "Supercritical Wing Sections III," *Lecture Notes in Economics and Mathematical Systems*, Vol. 150, Sringer-Verlag, New York, 1977.

[7] Stratford, B. S., "The Prediction of Separation of the Turbulent Boundary Layer," *Journal of Fluid Mechanics*, Vol. 5, 1959, pp. 1-16.

[8] McDonald, H. and Fish, R. W., "Practical Calculations of Transitional Boundary Layers," *International Journal of Heat and Mass Transfer*, Vol. 16, 1973, pp. 1729-1744.

[9] Starken, H., Breugelmans, F.A.E., and Schimming, P., "Investigation of the Axial Velocity Density Ratio in a High Turning Cascade," ASME Paper 75-GT-25, ASME Gas Turbine Conference and Products Show, Houston, Tex., March 1975.

[10] Ives, D. C. and Liutermoza, J. L., "Second Order Accurate Calculation of Transonic Flow Over Turbomachinery Cascades," AIAA Paper 78-1149, Seattle, Wash., July 1978.

[11] Ives, D. C. and Liutermoza, J. L., "Analysis of Transonic Cascade Flow Using Conformal Mapping and Relaxation Techniques," *AIAA Journal*, Vol. 15, May 1977, pp. 647-652.

[12] McNally, W. D., "Fortran Program for Calculating Compressible Laminar and Turbulent Boundary Layers in Arbitrary Pressure Gradients," NASA TN D-5681, May 1970.

[13] Roberts, W. B., "The Effect of Reynolds Number and Laminar Separation on Axial Cascade Performance," ASME Paper 74-GT-68, Nov. 1975.

[14] Lieblien, S. and Rouderbush, W. H., "Theoretical Loss Relations for Low Speed Two-Dimensional Cascade Flow," NACA TN 3662, March 1956.

[15] Stewart, W. L., "Analysis of Two-Dimensional Compressible Flow Loss Characteristics Downstream of Turbomachine Blade Rows in Terms of Basic Boundary Layer Characteristics," NACA TN 3515, July 1955.